ChemComm

Accepted Manuscript

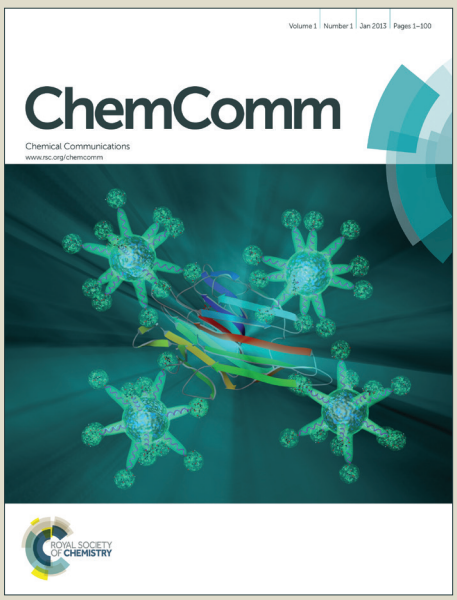

ROYAL SOCIETY OF CHEMISTRY

www.rsc.org/chemcomm

Cite this: DOI: 10.1039/c0xx00000x

www.rsc.org/xxxxxx

ARTICLE TYPE

Highly sensitive surface plasmon resonance sensor for the detection of DNA and cancer cell by target-triggered multiple signal amplification strategy

Peng He[1], Wenping Qiao[1], Lijun Liu[1], Shusheng Zhang[2]*

Received (in XXX, XXX) Xth XXXXXXXXX 20XX, Accepted Xth XXXXXXXXX 20XX
DOI: 10.1039/b000000x

A sensitive and versatile surface plasmon resonance bioassay was proposed for the detection of DNA and Ramos cell by combining the target-triggering isothermal exponential amplification with the magnetic nanoparticle-based rolling circle amplification, achieving remarkable amplification efficiency.

As the biomarker, DNA might provide useful information for the occurrence and development of some severe diseases such as cancers. In particular, the concentrations of relevant biomarkers are often present at a very low level in the early stage of disease. Thus, the detection of specific DNA sequences with extremely low abundance is important for gene therapy, mutation analysis and clinical diagnosis.[1] The polymerase chain reaction (PCR) assay is a traditional approach for amplifying specific target DNA, but it suffers from both insufficient specificity and thermal cycling.[2] Recently, surface plasmon resonance (SPR) biosensor has gained increasing attention due to fast, nondestructive and real-time detection of biological and chemical analytes.[3] Gold nanoparticles (AuNPs) are usually used in the SPR assay owing to their high density, large dielectric constant, and biocompatibility. So far, AuNP-based SPR assay has been widely applied for the detection of protein,[4] metal ions,[5] and small molecules,[6] as well as DNA.[7] However, the capability of SPR assay in the detection of DNA is limited by its relatively poor sensitivity due to the lack of powerful signal amplification methods.

As the alternative amplification techniques, isothermal amplification strategies, such as strand displacement amplification (SDA)[8] and exponential amplification reaction (EXPAR),[9] have been developed for the analysis of various target molecules by the combination with electrochemistry,[10] fluorescence,[11] colorimetry,[12] chemiluminescence,[13] and surface-enhanced Raman spectroscopy.[14] However, up to now, there are few reports about the combination of isothermal cycle amplification strategy with SPR assay.[15, 16] Recently, our group developed a SPR aptasensor combined with rolling circle amplification and bio-bar-coded AuNP enhancement for protein detection.[16] The strategy achieved ultrahigh sensitivity and showed excellent specificity. However, for the sandwich assay format, not all the target protein has two or more aptamers, which hampered its universal application.

Herein, on the basis of previous work, a novel and versatile SPR sensor was developed for sensitive detection of DNA by integrating multiple signal amplification strategy. Meanwhile, the proposed method was further successfully applied to the specific detection of cancer cells, demonstrating its potential application in early cancer diagnosis.

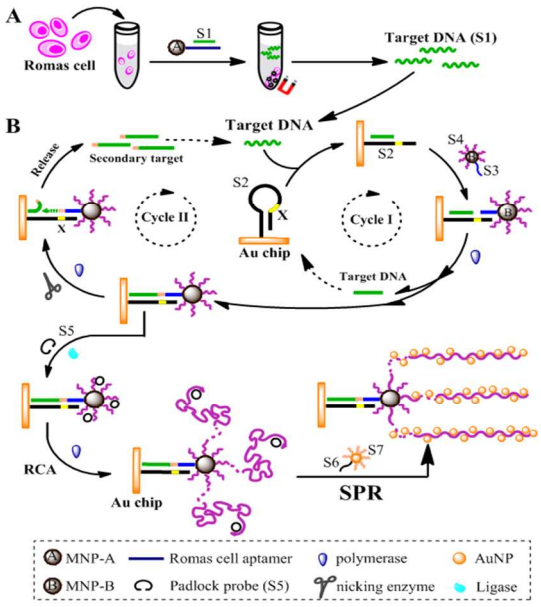

Scheme 1 Schematic representation of the multiple signal amplification SPR assay for DNA and cancer cell.

As shown in Scheme 1B, the proposed strategy for DNA assay includes the following three steps: (1) target-triggering isothermal exponential amplification reaction (T-EXPAR), (2) magnetic nanoparticle-based RCA reaction, and (3) AuNPs-enhanced SPR assay. In the first step, the amplification strategy is initiated by the hybridization of the target DNA (S1) with the loop region of the hairpin probe (S2) on the Au chip, thereby unfolding the

[1]*Key Laboratory of Sensor Analysis of Tumor Marker, Ministry of Education, College of Chemistry and Molecular Engineering, Qingdao University of Science and Technology, Qingdao 266042, P.R.China.*
[2]*College of Chemistry and Chemical Engineering, Linyi University, Linyi 276005, P. R. China. Fax : (+86) 532-84022700; Tel: (+86) 532-84022700; E-mail : shushzhang@126.com*
† Electronic Supplementary Information (ESI) available: Experimental procedures and additional figures. See DOI: 10.1039/b000000x/

hairpin probe. Next, DNA S3 on the bio-bar-code magnetic nanoparticle (MNP) as a primer anneals with the open stem and allows extension in the presence of Klenow DNA polymerase and dNTPs, which displaces the target DNA and forms a MNP bio-bar-code probe labeled DNA duplex. The displaced target DNA can bind another hairpin probe to initiate a new cycle of polymerization and displacement (SPD), constituting the target Cycle I in Scheme 1. The MNP bio-bar-code probe labeled DNA duplex produced from the Cycle I generates a recognition site (region X) for nicking enzyme. Subsequent single-stranded nicking produces a new replication site for the polymerase. As a result of strand-displacement activity of DNA polymerase, a large number of new single-stranded DNA (ssDNA) are generated through the repeated extension, cleavage, and release cycle. It should be noted that these released ssDNA are complementary with the hairpin probe, which can act as secondary target analogue to trigger the next reaction and initiate Cycle II. On the basis of the amplification reaction in Cycles I and II, the target DNA triggers can be exponentially produced, eventually leading to the generation of a large amount of MNP bio-bar-code probe labeled DNA duplex on Au chip. In the second step, after the circular template is formed by incubating the padlock probe S5 and T4 ligase on the DNA S4 of MNP bio-bar-code probe, the RCA reaction is initiated on the MNPs by adding DNA polymerase and dNTPs, producing hundreds of tandem-repeat sequences. In the third step, to efficiently avoid cross-reaction, bio-bar-code AuNPs are used as the detection probes and linearly and periodically assembled on the RCA products. The increasement of surface mass from clustered AuNPs conjugates on the SPR chip are real-time monitored by SPR biosensor. Through multiple signal amplification strategy, the SPR signal is significantly enhanced and the amplification efficiency correlates with the perfect matched the concentration of target DNA, providing a novel technique for the ultrasensitive detection of DNA.

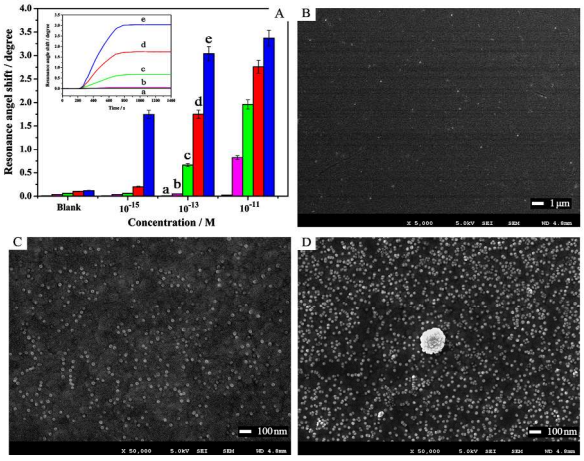

Fig. 1 (A) Comparison of SPR response of five different amplification formats: AuNP (a), AuNP-RCA (b), AuNP-MNP-RCA (c), AuNP-SPD-MNP-RCA (d) and AuNP-EXPAR-MNP-RCA (e). (B-D) SEM images of the SPR detection system for detection format a, b and e.

To prove the amplification efficiency of the multiple signal amplification strategy, five different amplification formats (a-e, Fig. S10- S17, ESI †) were studied for detection of the target DNA. As illustrated in Fig. 1A, a series of DNA solutions measured with SPR angular shifts for AuNP (format a), AuNP-RCA (format b), AuNP-MNP-RCA (format c), AuNP-SPD-MNP-RCA (format d) and AuNP-EXPAR-MNP-RCA (format e) amplification were compared. In the absence of the multiple amplification, the AuNP enhanced mode alone (format a) showed a limit of detection of about 10 pM for DNA, which is consistent with literature results.[7] Based on the each amplification step, the SPR signals for target DNA substantially enhance, but the background signals slightly increase. The high signal-to-noise ratio could also be obtained, which could be attributed to the inherent high selectivity of the hairpin DNA probes immobilized on the chip as well as the minimized non-specific adsorption by the effective surface blocking and washing. The inset of Fig. 1A shows real-time resonance angle responses with detection format a-e for 0.1 pM target DNA. For AuNP-MNP-RCA assay (c), the angular shift (~ 0.662°) was observed, which is about 16 times higher than that for Au-RCA format b (~ 0.04°). This enhancement is due to the employment of MNP bio-bar-code probe as the signal amplification intermediary, which can increase the coverage of the RCA product on the sensing surface. With the initiate of Cycle I mode (format d), SPR angle rapidly increased and the angle shift resulting from the attachment of AuNPs was about 1.75°. Based on the EXPAR assisted, the SPR response obtained with format e was significantly enhanced, which is about 1.7, 4.6 and 76 times higher than that with detection format d, c and b, respectively. The above results were further conformed by scanning electron microscope (SEM) images (Fig. 1B-D), which revealed the different aggregate phenomenon of AuNPs at 10 pM target DNA for detection format a, b and e. It is worth noting that in the presence of all signal amplification strategy, a large amount of AuNP could be generated on Au chip, showing the remarkable amplification performance of EXPAR, RCA and MNP enrichment.

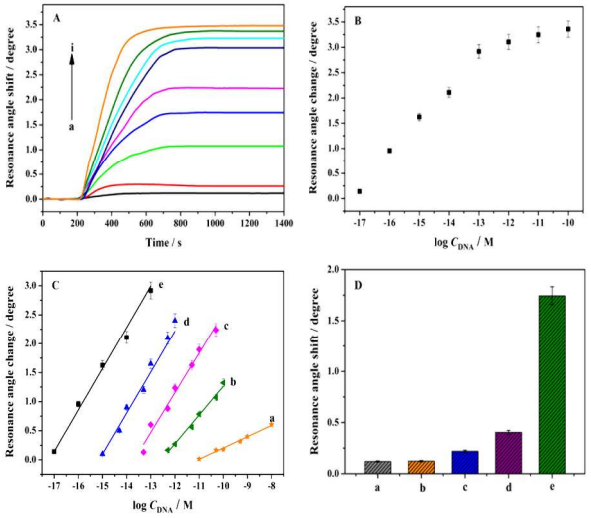

Fig. 2 (A) Real-time resonance angle responses of multiple amplified SPR biosensor for DNA detection. From a to i: 0, 10^{-17}, 10^{-16}, 10^{-15}, 10^{-14}, 10^{-13}, 10^{-12}, 10^{-11}, 10^{-10} M DNA. (B) SPR response curve for DNA detection using format e. (C) The calibration curves for DNA detection with amplification format a-e. (D) SPR response for blank (a), 1 fM of noncomplementary DNA S10 (b), two-base mismatched DNA S9 (c), single-base mismatched DNA S8 (d), perfect complementary target (e).

To evaluate the sensitivity of the proposed method, target DNA with different concentrations was measured under the optimal experimental conditions (Fig. S3- S9, ESI †). As shown in Fig. 2A, the real-time SPR angular shifts in response to AuNPs conjugates on the chip were observed with the increase in target DNA concentration. Fig. 2B shows the calibration curve of SPR signal with DNA concentration for AuNP-EXPAR-MNP-RCA amplification. The multiple amplified signal appears to show two segments of linear correlation to DNA concentration. From 0.1 pM to 0.1 nM, a relatively flat calibration curve was achieved due to the approximately saturated substrate and increasing steric inhibition. Another linear range is from 10 aM to 0.1 pM, which is more significant to ultrasensitive detection of target DNA. The regression equation was $Y = 0.7131 \log C + 12.2659$ (Y is the SPR angular shift after subtracting the response of the blank solution and C is the concentration of DNA), with a correlation coefficient of 0.9969 (Fig. 2C, e). The calibration curves for the detection of DNA by using detection format a-d are also plotted in Fig. 2C. The limit of detection (LOD) for each format was obtained by evaluating the average response of the negative control plus 3 times standard deviation. Notably, the LOD for multiple amplification strategy (e) is 9.3 aM, which is much lower than detection format a (10 pM), detection format b (0.35 pM), detection format c (45 fM), detection format d (1 fM), and competitive with many reported method (Table S3, ESI †) such as PCR-based SPR method (150 nM).[17] This low detection limit might be attributed to the high amplification efficiency of circular T-EXPAR, MNP-based RCA and AuNP enhancement (Table S2, ESI †).

The specificity of DNA assay was further investigated. As shown in Fig. 2D, no apparent change in the SPR angular shift was observed with the non-complementary DNA, compared with the blank test. The SPR responses for the two-base mismatched DNA S9 and single-base mismatched DNA S8 were only about 12.6% and 23.2% of that for perfect complementary target DNA, respectively. These results clearly demonstrate the good selectivity of this method.

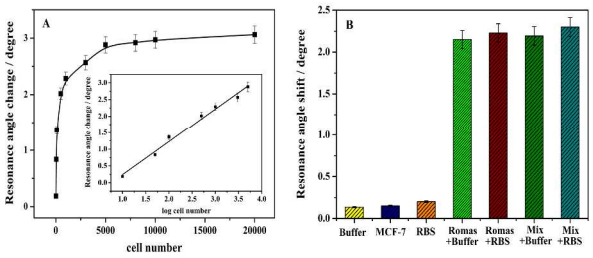

Fig. 3 (A) SPR response curve for Ramos cells detection using AuNP-EXPAR-MNP-RCA amplification. (B) The specificity of the multiple signal amplification assay for Romas cells.

The amplification strategy for cancer cells assay was proposed based on specific recognition and high affinity of aptamers to cell, using the above mentioned DNA amplified detection protocol. The principle of the strategy is shown in Scheme 1A. The Ramos cell aptamer is immobilized on the surface of MNP-A. DNA S1 hybridizes with the cell aptamer, forming a rigid duplex aptamer probes on MNP-A. In the presence of the Ramos cells, Ramos cells interact with aptamer probes to form the MNP-aptamer-cell complex, resulting in the disassembly of the original duplex and the release of DNA S1. It is the released DNA S1 that acts as target DNA to enter into the DNA amplification system and trigger the next reaction. The following processes are the same as Scheme 1B. Fig. 3A shows the SPR signals increase with increasing number of Ramos cells. The SPR angular change has a linear relationship with the logarithm of Romas cell number in the range from 10 to 5000 cells (inset of Fig. 3A). The regression equation is $Y = 0.9868 \log N - 0.7449$ with a correlation coefficient of 0.9948, where Y is the SPR angular change and N is the number of cells. A detection limit of 10 cells can be estimated using 3σ. The specificity, matrix effect and practicality were further investigated. Based on the highly specific binding of aptamer to target cell and efficient magnetic separation, the SPR signal responding to MCF-7 cell was similar to that of blank buffer (Fig. 3B). Comparable responses were obtained for Romas cell in both buffer and real blood sample (RBS). The background signal obtained in RBS was slightly higher than that in buffer, which is probably due to the interferences of the complex matrices. The amount of Romas cell spiked in RBS was evaluated and the recovery was found to vary from 91.5 to 97.8% (Table S4, ESI†). These results demonstrated the feasibility and versatility of this platform in clinical diagnosis and point-of-care use.

In summary, a SPR strategy was developed for detection of DNA and cancer cells by combining target-triggered cascade signal amplification and AuNP enhancement. Although this method is relatively complex, the experimental operation is robust, isothermal and cost-effective. More importantly, the proposed assay exhibited a broad dynamic range, ultrahigh sensitivity and excellent specificity. This assay represents a novel technique for both qualitative and quantitative detection of cancer cells in the blood sample, holding great promise for the broad applications in the field of medical research.

This work was supported by the National Natural Science Foundation of China (21227008, 21275086, 21025523).

Notes and references

1 (a) N. L. Rosi, D. A. Giljohann, C. S. Thaxton, A. K. R. Lytton-Jean, M. S. Han, C. A. Mirkin, *Science*, 2006, **312**, 1027; (b) W. Xu, X. Xue, T. Li, H. Zeng, X. Liu, *Angew. Chem., Int. Ed.*, 2009, **48**, 6849.

2 (a) J. Mulder, N. McKinney, C. Christopherson, J. Sninsky, L. Greenfield, S. Kwok, *J. Clin. Microbiol.*, 1994, **32**, 292; (b) D. A. Giljohann, C. A. Mirkin, *Nature*, 2009, **462**, 461.

3 (a) B. A. Snopok, Theoretical and Experimental Chemistry, 2012, 48, 283; (b) S. Krishnan, V. Mani, D. Wasalathanthri, C. V. Kumar, J. F. Rusling, *Angew. Chem. Int. Ed.*, 2011, **50**, 1175; (c) L. Wang, C. Zhu, L. Han, L. Jin, M. Zhou, S. Dong, *Chem. Commun.*, 2011, **47**, 7794; (d) P. M. Boltovets, O. M. Polischuk, O. G. Kovalenko, B. A. Snopok, *Analyst*, 2013, **138**, 480.

4 (a) Y. Uludag, I. E. Tothill, *Anal. Chem.*, 2012, **84**, 5898; (b) Y. F. Bai, F. Feng, L. Zhao, C. Y. Wang, H. Y. Wang, M. Z. Tian, J. Qin, Y. L. Duan, X. X. He, *Biosens. Bioelectron.*, 2013, **47**, 265.

5 E. J. Kim, B. H. Chung, H. J. Lee, *Anal. Chem.*, 2012, **84**, 10091.

6 J. Wang, H. S. Zhou, *Anal. Chem.*, 2008, **80**, 7174.

7 (a) L. He, M. D. Musick, S. R. Nicewarner, F. G. Salinas, S. J. Benkovic, M. J. Natan, C. D. Keating, *J. Am. Chem. Soc.*, 2000, **122**, 9071; (b) M. Hayashida, A. Yamaguchi, H. Misawa, *Jpn. J. Appl. Phys., Part 2*, 2005, **44**, L1544.

8 (a) A. R. Connolly, M. Trau, *Angew. Chem. Int. Ed.*, 2010, **49**, 2720; (b) Q. P. Guo, X. H. Yang, K. M. Wang, W. H. Tan, W. Li, H. X. Tang, H. M. Li, *Nucleic Acids Res.*, 2009, **37**, e20.

9 (a) H. X. Jia, Z. P. Li, C. H. Liu, Y. Q. Cheng, *Angew. Chem. Int. Ed.*, 2010, **49**, 5498; (b) Y. Zhang, C. Y. Zhang, *Anal. Chem.*, 2012, **84**, 224.

10 (a) Y. Cao, S. Zhu, J. Yu, X. Zhu, Y. Yin, G. Li, *Anal. Chem.*, 2012, **84**, 4314; (b) J. Nie, D. Zhang, F. Zhang, F. Yuan, Y. Zhou, X. Zhang, *Chem. Commun.*, 2014, **50**, 6211.

11 (a) H. Zhou, S. Xie, S. Zhang, G. Shen, R. Yu, Z. Wu, *Chem. Commun.*, 2013, **49**, 2448; (b) Y. Zhang, L. Wang, C. Zhang, *Chem. Commun.*, 2014, **50**, 1909.
12 (a) J. Li, H. Fu, L. Wu, A. Zheng, G. Chen, H. Yang, *Anal. Chem.*, 2012, **84**, 5309; (b) L. Tang, Y. Liu, M. M. Ali, D. K. Kang, W. Zhao, J. Li, *Anal. Chem.*, 2012, **84**, 4711.
13 L. Wang, Y. Zhang, C. Zhang, *Anal. Chem.*, 2013, **85**, 11509.
14 (a) P. He, Y. Zhang, L. Liu, W. Qiao, S. Zhang, *Chem. Eur. J.*, 2013, **19**, 7452; (b) J. Hu, C. Zhang, *Anal. Chem.*, 2010, **82**, 8991.
15 Y. Xiang, K. Deng, H. Xia, C. Yao, Q. Chen, L. Zhang, Z., W. Fu, *Biosens. Bioelectron.*, 2013, **49**, 442.
16 P. He, L. Liu, W. Qiao, S. Zhang, *Chem. Commun.*, 2014, **50**, 1481.
17 E. Kai, S. Sawata, K. Ikebukuro, T. Iida, T. Honda, I. Karube, *Anal. Chem.*, 1999, **71**, 796.